SCIENCE CHINA
Information Sciences

• RESEARCH PAPER •

February 2017, Vol. 60 022312:1–022312:12
doi: 10.1007/s11432-016-0452-x

Upper bounds on the capacity for optical intensity channels with AWGN

Yingying YU, Zaichen ZHANG*, Liang WU & Jian DANG

National Mobile Communications Research Laboratory, Southeast University, Nanjing 210096*, China*

Received August 15, 2016; accepted September 17, 2016; published online December 16, 2016

Abstract The channel capacity of the optical wireless communication (OWC) systems is still a problem that has not an optimal and close-form expression, in spite of OWC can be used to achieve high data rates. This paper presents novel upper bounds on the channel capacity of an optical intensity modulated and directed detection (IM/DD) system under peak-power and average-power constraints. The channel is modeled as an additive white Gaussian noise (AWGN) optical channel. The bounds are derived based on sphere-based signal space argument. Simulation results show the proposed bounds are tight at both high and low signal-to-noise ratios (SNRs). Compared to those reported bounds, the derived bounds are better at high SNRs region in particular, and the expressions are simpler and unique for the whole range of average-to-peak-power ratio.

Keywords channel capacity, optical communication, AWGN, sphere-based signal space, high signal-to-noise ratios (SNRs)

Citation Yu Y Y, Zhang Z C, Wu L, et al. Upper bounds on the capacity for optical intensity channels with AWGN. Sci China Inf Sci, 2017, 60(2): 022312, doi: 10.1007/s11432-016-0452-x

1 Introduction

The channel capacity is a focus in research of the optical wireless communication (OWC) systems. Although real amplitude or phase modulation [1,2] is used in conventional wireless mobile systems, intensity modulated and direct detection (IM/DD) and wavelength division multiplexed (WDM) [3, 4] are often considered for practical, low-cost system implementations in OWC systems. Therefore, the results of the channel capacity in wireless mobile systems cannot be used in OWC systems directly. Information in OWC systems is modulated as the instantaneous optical intensity. Furthermore, the average optical power, i.e., average amplitude for optical signal, is restricted to meet eye safety standards and the power consumption requirements of device.

Regarding to the channel model with IM/DD, there are two different methods for constructing the optical channels — Poisson channels (see, e.g., [5–11]) and additive white Gaussian noise (AWGN) channels (see, e.g., [12–21]). In the former case, the quantum property of the transmitted signal and of the dominant noise source is reflected by consisting of many photons, which is a physical nature of the optical signal. The channel law is treated as a Poisson statistics process. An additional constant caused by background noise reduces the accurate number of arriving photons at the receiver. The AWGN channel is

* Corresponding author (email: zczhang@seu.edu.cn)

modeled as a linear channel with zero-mean and signal-independent Gaussian noise, just like the AWGN channel in radio frequency (RF) systems. The different behaviors of channel capacity of the two channels are discussed in [14].

Compared to the Poisson channels, it is more difficult to find an accurate and close-form solution of the capacity for AWGN channels. Rather than the close-form solution, the tighter upper bounds and lower bounds are more practical. In [22], the sphere-based signal space argument was proposed. The argument can be available to obtain an upper capacity bound for the AWGN optical channels, which can be found in some literature. In [15], the upper capacity bounds for optical channels in both pulse amplitude modulation (PAM) systems and quadrature amplitude modulation (QAM) systems were presented. In [16], the upper bounds with limited band and limited power were derived, but difference between the upper bounds and the lower bounds is not small. In [17–19], some better results of the optical intensity channels were given. However, they did not consider the peak-power constraint, and the bounds were not tight enough for both low and high signal-to-noise ratios (SNRs).

In this paper, we derive a tighter upper bound on the capacity under average-power and peak-power constraints, and study the corresponding asymptotic behaviors at high and low average-power values. The bound is solved by the sphere-based signal space argument. The paper is organized as follows. An AWGN channel model of the optical communication systems is established in Section 2. The results of the capacity bounds are presented in Section 3. The numerical analysis and performance discussion of the bounds are carried out in Section 4. Some simulation examples and interpretations for the derived bounds are shown in Section 5. Finally, conclusions are presented in Section 6.

2 System model

The thermal noise and the shot noise are the dominant noise sources in OWC systems. In AWGN channels, the noise can be assumed to be Gaussian distributed, independent of transmitted optical signal. Then, for $t \in [0, T), T > 0$, a representation can be written as [15, 23]

$$y(t) = Rx(t) \otimes h(t) + z(t), \tag{1}$$

where symbol $\otimes$ denotes the convolution operation, R is the photodiode responsivity and without loss of generality, we set $R = 1$ in this paper, $h(t)$ is the channel impulse response and we assume the channel is frequency nonselective (i.e., $h(t) = H\delta(t)$), $z(t)$ is AWGN with zero-mean and variance σ^2, $x(t)$ is the transmitted instantaneous optical intensity signal and must satisfy [12, 23, 24]

$$0 \leqslant x(t) \leqslant A, \tag{2}$$

$$E[x(t)] \leqslant P_0 \tag{3}$$

with $A > 0$ and $P_0 > 0$ being the allowed values of the peak-power and the average-power constraints, respectively.

Under the above assumptions, we can redefine the transmitted signal combined with the channel response as $v(t) = H \cdot x(t)$ and rewrite the channel model in a vector form with a set of N-dimensional orthonormal basis functions as [16, 22]

$$\mathbf{Y} = \mathbf{V} + \mathbf{Z}. \tag{4}$$

The constraints (2) and (3) can be transformed into

$$0 \leqslant |\mathbf{V}| \leqslant AH, \tag{5}$$

and

$$E[\mathbf{V}] \leqslant HP_0, \tag{6}$$

where the $|\cdot|$ denotes a vector norm.

The following results are given for our derivation. We would rather only state than describe them in detail. For more details, see [16, 17].

Proposition 1. Consider transmitting a series of M-dimensional independent symbols to form a codeword $\mathbf{x} = (x_1, x_2, \cdots, x_M)$. Geometrically, the admissible region of transmitted codewords Θ, under nonnegativity and average amplitude constraints, forms the regular M-simplex:

$$\Theta = \left\{ \mathbf{x} \in \mathbb{R}^M : \forall m, x_m \geqslant 0, \frac{1}{M} \sum_{m=1}^{M} x_m \leqslant P_0 \right\}.$$

For M large enough, the channel capacity is upper-bounded by

$$C \leqslant \lim_{M\to\infty} \frac{1}{M} \log_2 \frac{V(\Theta)}{V(rB^M)} = \lim_{M\to\infty} \frac{1}{M} \log_2 \frac{V(\Theta)}{r^M \cdot V(B^M)}, \tag{7}$$

where $V(\cdot)$ represents the volume of the region, $r = \sqrt{M\sigma^2}$, B^M is the M-dimensional unit ball and can be written as

$$V\left(B^M\right) = \frac{\pi^{M/2}}{\Gamma(M/2+1)} = \begin{cases} \dfrac{\pi^k}{k!}, & M = 2k, \\ \dfrac{2(k!)(4\pi)^k}{(2k+1)!}, & \text{otherwise}, \end{cases} \quad k \in \mathbb{N}. \tag{8}$$

Proposition 2.

$$\lim_{M\to\infty} \max_u f(u, M) = \max_u \lim_{M\to\infty} f(u, M). \tag{9}$$

3 Channel capacity bounds

The derivation of the upper bounds in the following is based on the geometric characteristics of signal space. We employ the expression of intrinsic volumes of a polynomial in [25] to analyze the upper bounds. The volume $V(\Theta)$ can be given by

$$V(\Theta) = \sum_{\substack{i=kN+1 \\ k=0,1,\cdots,(M-1)}} V_i V\left(B^{MN-i}\right) r^{MN-i}, \tag{10}$$

where $r = \sqrt{MN\sigma^2}$, V_i is the intrinsic volume and can be expressed as

$$V_i = \begin{cases} \dfrac{\kappa_i \chi^i}{i!}, & i = kN+1; k = 0, 1, \cdots, (M-1), \\ 0, & \text{otherwise}, \end{cases} \tag{11}$$

with χ being the length of volume of the body Θ,

$$\kappa_i = \begin{cases} \dbinom{MN}{i} \dfrac{1}{2^{MN-i}} + \dbinom{MN}{i+1} \dfrac{i+1}{\sqrt{\pi}} \displaystyle\int_0^\infty \mathrm{e}^{-(i+1)t^2} \left(\frac{1+\operatorname{erf}(t)}{2}\right)^{MN-i-1} dt, & 0 \leqslant i \leqslant MN-1, \\ 1, & i = MN, \end{cases} \tag{12}$$

where $\operatorname{erf}(x) = \frac{2}{\sqrt{\pi}} \int_0^x \mathrm{e}^{-z^2} dz$ is the error function.

Lemma 1. For the average-to-peak-power ratio $\rho = \frac{P_0}{A}$, the upper capacity bounds for optical channels under average-power and peak-power constraints can be distinguished between two cases: $0 < \rho < 1$ and $\rho = 1$.

Proof. See Appendix A for the detailed proof.

Next, we will discuss the upper bounds on the capacity in the two ranges in detail. It is noted that the bounds are discussed equivalently only under the peak-power constraint in the case of $\rho = 1$ [12].

3.1 In case of $0 < \rho < 1$

In the range of $0 < \rho < 1$, the boundary in $\chi = \frac{HP_0\sqrt{MT}}{\cos\beta}$ and β is defined by (A8). The volume $V(\Theta)$ can be rewritten as

$$V(\Theta) = \sum_{\substack{i=kN+1 \\ k=0,1,\cdots,(M-1)}} \frac{\kappa_i}{i!}\left(MHP_0\sqrt{T}\right)^i V\left(B^{MN-i}\right) r^{MN-i}. \tag{13}$$

For the purpose of a more immediate upper bound of the optical channel capacity, the coefficient κ_i in the rang of $0 \leqslant i \leqslant MN-1$ is upper bounded as (the derivation is presented in Appendix B)

$$\kappa_i \leqslant \begin{pmatrix} MN+1 \\ i+1 \end{pmatrix} \frac{\sqrt{i+1}}{2}. \tag{14}$$

Substituting into (13) and (14), the capacity upper bound (7) can be rewritten as

$$C \leqslant \lim_{M\to\infty} \frac{1}{M}\log_2 \frac{V(\Theta)}{r^{MN}\cdot V\left(B^{MN}\right)} \tag{15a}$$

$$\leqslant \lim_{M\to\infty} \frac{1}{M}\log_2 \sum_{\substack{i=kN+1 \\ k=0,1,\cdots,(M-1)}} \left[f_i \frac{\sqrt{i+1}}{2r^i i!}\frac{V\left(B^{MN-i}\right)}{V\left(B^{MN}\right)}\right] \tag{15b}$$

$$\leqslant \lim_{M\to\infty} \frac{1}{M}\max_i \log_2 F_1(MN) \tag{15c}$$

$$= \lim_{M\to\infty} \frac{1}{M}\max_u \log_2 G_1(MN) \tag{15d}$$

$$= \max_u \log_2 \left[\frac{(1-u)^{\frac{3N(u-1)}{2}}}{u^{2uN}}\left(\frac{HP_0\sqrt{T}}{\sigma N\sqrt{\mathrm{e}\pi}}\right)^{uN}\right], \tag{15e}$$

where

$$f_i = \begin{pmatrix} MN+1 \\ i+1 \end{pmatrix}\left(MHP_0\sqrt{T}\right)^i,$$

$$F_1(MN) = \left(\frac{MN+1+\mathrm{b}}{MN-i+\mathrm{a}}\right)^{MN}\left(\frac{M}{i+\mathrm{a}}\right)^i\left(\frac{MN+2\mathrm{c}}{MN-i+2\mathrm{a}}\right)^{\frac{MN}{2}} \times \left(\frac{HP_0\sqrt{T}}{\sigma N\sqrt{\mathrm{e}\pi}}\right)^i\left(\frac{MN-i+\mathrm{a}}{i+1+\mathrm{a}}\right)^i\left(\frac{(MN-i)/2+\mathrm{a}}{MN}\right)^{i/2}$$

with $\mathrm{a} = 1/2, \mathrm{b} = \mathrm{e}^{1-\gamma}-1, \mathrm{c} = \mathrm{e}^{-\gamma}$, and γ being the Euler-Mascheroni constant,

$$G_1(MN) = \left(\frac{MN+1+\mathrm{b}}{(1-u)MN+uN-1+\mathrm{a}}\right)^{MN}\left(\frac{MHP_0\sqrt{T}}{(uMN-uN+1+\mathrm{a})\sigma N\sqrt{\mathrm{e}\pi}}\right)^{uMN-uN+1} \times \left(\frac{MN+2\mathrm{c}}{(1-u)MN+uN-1+2\mathrm{a}}\right)^{\frac{MN}{2}}\left(\frac{(1-u)MN+uN-1+\mathrm{a}}{uMN-uN+2+\mathrm{a}}\right)^{uMN-uN+1} \times \left(\frac{((1-u)MN+uN-1)/2+\mathrm{a}}{MN}\right)^{\frac{uMN-uN+1}{2}}.$$

The derivation of (15c) is proved in Appendix C. Eq. (15d) can be solved by defining

$$i = \lfloor u(M-1)\rfloor N+1,\ 0 \leqslant u \leqslant 1, \tag{16}$$

where $\lfloor\cdot\rfloor$ denotes the floor operation.

3.2 In case of $\rho = 1$

When $\rho = 1$, $\chi = (M-1)\,HA\sqrt{T}$ and the volume $V(\Theta)$ can be rewritten as

$$V(\Theta) = \sum_{\substack{i=kN+1 \\ k=0,1,\cdots,(M-1)}} \frac{\kappa_i}{i!}\left((M-1)\,HA\sqrt{T}\right)^i V\left(B^{MN-i}\right) r^{MN-i}. \tag{17}$$

Substituting into (17) and (14), the capacity upper bound (7) can be rewritten as

$$C \leqslant \lim_{M\to\infty} \frac{1}{M}\log_2 \sum_{\substack{i=kN+1 \\ k=0,1,\cdots,(M-1)}} \left[g_i \frac{\sqrt{i+1}}{2r^i i!}\frac{V\left(B^{MN-i}\right)}{V\left(B^{MN}\right)}\right] \tag{18a}$$

$$\leqslant \lim_{M\to\infty} \frac{1}{M}\max_i \log_2 F_2(MN) \tag{18b}$$

$$= \lim_{M\to\infty} \frac{1}{M}\max_u \log_2 G_2(MN) \tag{18c}$$

$$= \max_u \log_2 \left[\frac{(1-u)^{\frac{3N(u-1)}{2}}}{u^{2uN}}\left(\frac{HP_0\sqrt{T}}{\sigma N\sqrt{\mathrm{e}\pi}}\right)^{uN}\right], \tag{18d}$$

where

$$g_i = \binom{MN+1}{i+1}\left((M-1)\,HA\sqrt{T}\right)^i,$$

$$F_2(MN) = M\left(\frac{MN+1+\mathrm{b}}{MN-i+\mathrm{a}}\right)^{MN}\left(\frac{M-1}{i+\mathrm{a}}\right)^i\left(\frac{MN+2\mathrm{c}}{MN-i+2\mathrm{a}}\right)^{\frac{MN}{2}} \times \left(\frac{HA\sqrt{\mathrm{e}T}}{\sigma N\sqrt{\pi}}\right)^i\left(\frac{MN-i+\mathrm{a}}{i+1+\mathrm{a}}\right)^i\left(\frac{(MN-i)/2+\mathrm{a}}{MN}\right)^{i/2},$$

$$G_2(MN) = M\left(\frac{MN+1+\mathrm{b}}{(1-u)\,MN+uN-1+\mathrm{a}}\right)^{MN}\left(\frac{(M-1)\,HA\sqrt{\mathrm{e}T}}{(uMN-uN+1+\mathrm{a})\,\sigma N\sqrt{\pi}}\right)^{uMN-uN+1} \times \left(\frac{MN+2\mathrm{c}}{(1-u)\,MN+uN-1+2\mathrm{a}}\right)^{\frac{MN}{2}}\left(\frac{(1-u)\,MN+uN-1+\mathrm{a}}{uMN-uN+2+\mathrm{a}}\right)^{uMN-uN+1} \times \left(\frac{((1-u)\,MN+uN-1)/2+\mathrm{a}}{MN}\right)^{\frac{uMN-uN+1}{2}}.$$

The derivation can be shown from the previous section.

In summary, the channel capacity can then be bounded as

$$\mathrm{C_{UB}} = \max_u \log_2\left[(1-u)^{\frac{3N(u-1)}{2}}u^{-2uN}d_0^{uN}\right], \tag{19}$$

where

$$d_0 = \frac{HP_0\sqrt{T}}{\sigma N\sqrt{\mathrm{e}\pi}}. \tag{20}$$

To find the optimal solution of (19), we define L_1 as follows:

$$L_1 = \frac{3uN-3N}{2}\ln(1-u) - 2uN\ln(u) + uN\ln(d_0). \tag{21}$$

Then the problem (19) can be transformed into

$$\max_u L_1, \text{ when } 0 \leqslant u \leqslant 1.$$

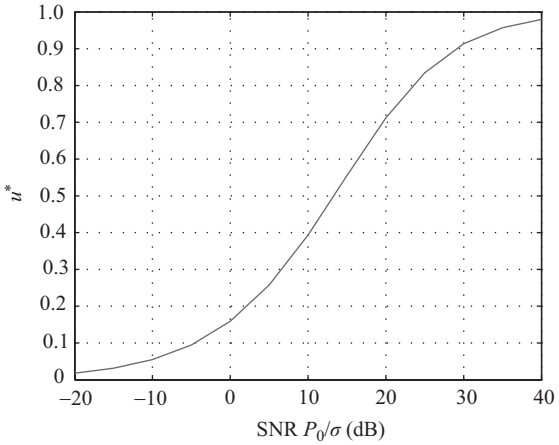

Figure 1 Optimum u^* given in (24) for SNRs.

It shows obviously that L_1 is concave in the given interval of u since $\frac{\partial^2}{\partial u^2}L_1 = -\frac{3}{1-u} - \frac{4}{u} < 0$, i.e., the maximum value can be solved by setting $\frac{\partial}{\partial u}L_1 = 0$. The optimal u^* can be obtained as the solution of

$$\eta_1(u^*) = 3\ln(1-u^*) - 4\ln(u^*) - 1 + 2\ln(d_0) = 0, \tag{22}$$

or

$$\eta_1'(u^*) = \mathrm{e}(u^*)^4 + d_0^2(u^*)^3 - 3\,d_0^2(u^*)^2 + 3\,d_0^2u^* - d_0^2 = 0. \tag{23}$$

In $0 \leqslant u \leqslant 1$, $\frac{\partial}{\partial u}\eta_1'(u) > 0$. Then, $\eta_1'(u)$ is monotone increasing. In addition, $\eta_1'(0) = -d_0^2 < 0$ and $\eta_1'(1) = \mathrm{e} > 0$. Therefore, there is only one root for $\eta_1'(u)$ in $[0,1]$ and the root is

$$u^* = -\frac{d_0^2}{4\mathrm{e}} - \frac{1}{2}\sqrt{\frac{d_0^4}{4\mathrm{e}^2} + 2\frac{d_0^2}{\mathrm{e}} + o} + \frac{1}{2}\sqrt{\frac{d_0^4}{2\mathrm{e}^2} + 4\frac{d_0^2}{\mathrm{e}} - o + \frac{\frac{d_0^6}{\mathrm{e}^3} + 12\frac{d_0^4}{\mathrm{e}^2} + 24\frac{d_0^2}{\mathrm{e}}}{4\sqrt{\frac{d_0^4}{4\mathrm{e}^2} + 2\frac{d_0^2}{\mathrm{e}} + o}}}, \tag{24}$$

where

$$o = \frac{d_0}{\mathrm{e}}\left[\frac{\mathrm{e}d_0}{2} + \frac{\mathrm{e}}{2}\left(\frac{256}{27}\mathrm{e} + d_0^2\right)^{\frac{1}{2}}\right]^{\frac{1}{3}} - \frac{4\,d_0}{3}\left[\frac{\mathrm{e}d_0}{2} + \frac{\mathrm{e}}{2}\left(\frac{256}{27}\mathrm{e} + d_0^2\right)^{\frac{1}{2}}\right]^{-\frac{1}{3}}.$$

Theorem 1. The upper capacity bound for the optical channels under peak-power and average-power constraints can be written as

$$\mathrm{C_{UB}} = \log_2\left[d_0^{Nu^*}\frac{(1-u^*)^{3N(u^*-1)/2}}{(u^*)^{2Nu^*}}\right], \tag{25}$$

where N is the dimensionality of the orthogonal decomposition of transmitted signal, d_0 and u^* are defined by (20) and (24), respectively.

It is noted that u^* tends to be zero and one as P_0 tends to be negative infinity and infinity, respectively. The behavior of u^* versus SNR (defined as $\frac{P_0}{\sigma}$) is shown in Figure 1. Hence, the asymptotic expansions for the channel capacity upper bound in the two regions are

Corollary 1.

$$\lim_{P_0\to\infty}\{\mathrm{C_{UB}} - N\log_2 d_0\} = 0 \tag{26}$$

and

$$\lim_{P_0\downarrow 0}\frac{\mathrm{C_{UB}}}{d_0^{1/3}} = 0. \tag{27}$$

Proof. See Appendix E for the detailed proof.

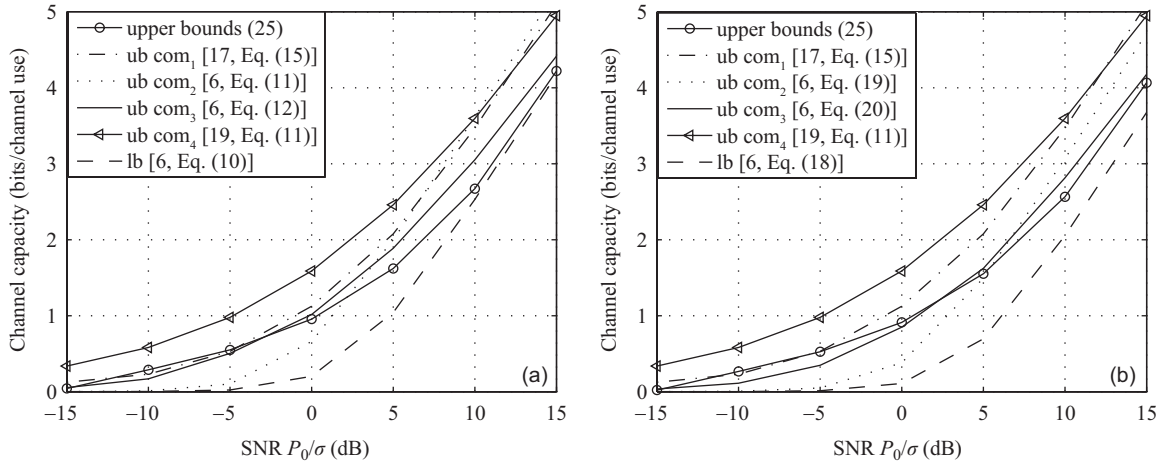

Figure 2 Comparison of capacity bounds for different ρ. (a) $\rho = 0.4$; (b) $\rho = 0.6$ ($T = 1$ in all cases [22]).

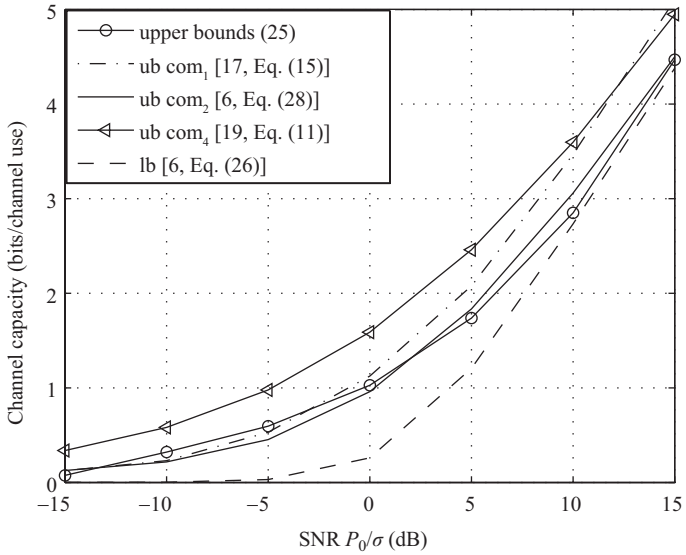

Figure 3 Comparison of capacity bounds with average-power constraint only ($T = 1$ in all cases [22]).

4 Simulation results

Next, we present several simulation results to verify the performance of the proposed upper bound under various scenarios. The upper bound, $\mathrm{C_{UB}}$ in (25), versus SNR is shown in Figure 2 for different power ratio ρ and $N = 2$. For comparison, the upper bounds in [12,17,19] and the lower bounds in [12] are also plotted in Figure 2. In addition, a case without the peak-power constraint is shown in Figure 3, which has the same upper bound with the previous case with the peak-power and average-power constraints of the proposed result. Notice that $\mathrm{C_{UB}}$ provides a significantly better upper bound for the channel capacity than the previous upper bounds, especially at high SNR, i.e., SNR $>$ 0 dB. At low SNR, upper bounds ((11), (19) and (28)) in [12] can obtain the tightest upper bounds. The main reason may be that the bounds in [12] rely on the choice of the distribution on the output — a clever choice can lead to a good bound. However, it is hard to find such a choice which can be good for the whole range of SNR. Besides, the unique expression pattern of the proposed bound in different cases of the average-to-peak-power ratio is simpler than these results.

5 Conclusion

A new and unique expression of the upper bound on the capacity of optical intensity channels with a peak-power constraint and an average-power constraint was derived based on sphere-based signal space argument. For a fixed ratio of the average-power to the peak-power, the gap between the upper bound and the existing tighter lower bound (see, [12]) goes to small at high SNR. Besides, we also get the asymptotic expansions of the upper bound in the two regions of the average-power constraint — infimum and infinity.

Acknowledgements This work was supported by National Natural Science Foundation of China (Grant Nos. 61501109, 61571105, 61223001), National High Technology Research and Development Program of China (863) (Grant No. 2013AA013601), and Jiangsu National Science Foundation (Grant No. BK20140646).

Conflict of interest The authors declare that they have no conflict of interest.

References

1 Zhu H, Wang J. Chunk-based resource allocation in OFDMA systems - part I: chunk allocation. IEEE Trans Commun, 2009, 57: 2734–2744
2 Zhu H, Wang J. Chunk-based resource allocation in OFDMA systems - part II: joint chunk, power and bit allocation. IEEE Trans Commun, 2012, 60: 499–509
3 Zhao D, Long K, Zheng Y, et al. Channel power control in optical amplifiers to mitigate physical impairment in optical network. Sci China Inf Sci, 2015, 58: 022302
4 Huang S, Zhang Y, Sun L, et al. A load balancing multi-path routing scheme based on effective voids for optical burst switching networks. Sci China Inf Sci, 2015, 58: 102305
5 Lapidoth A, Moser S M. On the capacity of the discrete-time Poisson channel. IEEE Trans Inf Theory, 2009, 55: 303–322
6 Wang L, Wornell G W. A refined analysis of the Poisson channel in the high-photon-efficiency regime. IEEE Trans Inf Theory, 2014, 60: 4299–4311
7 Lapidoth A, Shapiro J H, Venkatesan V, et al. The discrete-time Poisson channel at low input powers. IEEE Trans Inf Theory, 2011, 57: 3260–3272
8 Lai L, Liang Y, Shitz S S. On the capacity bounds for Poisson interference channels. IEEE Trans Inf Theory, 2015, 61: 223–238
9 Aisha A, Lai L, Liang Y. Optimal power allocation for Poisson channels with time-varying background light. IEEE Trans Commun, 2015, 63: 4327–4338
10 Alem-Karladani M M, Sepahi L, Jazayerifar M, et al. Optimum power allocation in parallel Poisson optical channel. In: Prococeedings of International Conference on Telecommunications, Zagreb, 2009. 285–288
11 Martinez A. Spectral efficiency of optical direct detection. J Opt Soc Amer B, 2007, 24: 739–749
12 Lapidoth A, Moser S M, Wigger M A. On the capacity of free-space optical intensity channels. IEEE Trans Inf Theory, 2009, 55: 4449–4461
13 Agrell E, Alvarado A, Durisi G, et al. Capacity of a nonlinear optical channel with finite memory. J Lightwave Technol, 2014, 32: 2862–2876
14 Moser S M. Capacity results of an optical intensity channel with input-dependent Gaussian noise. IEEE Trans Inf Theory, 2012, 58: 207–223
15 You R, Kahn J M. Upper-bounding the capacity of optical IM/DD channels with multiple-subcarrier modulation and fixed bias using trigonometric moment space method. IEEE Trans Inf Theory, 2002, 48: 514–523
16 Hranilovic S, Kschischang F R. Capacity bounds for power- and band-limited optical intensity channels corrupted by Gaussian noise. IEEE Trans Inf Theory, 2004, 50: 784–795
17 Wang J B, Hu Q S, Wang J, et al. Tight bounds on channel capacity for dimmable visible light communications. J Lightwave Technol, 2013, 31: 3771–3779
18 Farid A A, Hranilovic S. Capacity bounds for wireless optical intensity channels with Gaussian noise. IEEE Trans Inf Theory, 2010, 56: 6066–6077
19 Jiang R, Wang Z, Wang Q, et al. A tight upper bound on channel capacity for visible light communications. IEEE Commun Lett, 2016, 20: 97–100
20 Wang Q, Wang Z, Dai L. Asymmetrical hybrid optical OFDM for visible light communications with dimming control. IEEE Photonics Technol Lett, 2015, 27: 974–977
21 Armstrong J. OFDM for optical communications. J Lightwave Technol, 2009, 27: 189–204
22 Hranilovic S, Kschischang F R. Optical intensity-modulated direct detection channels: signal space and lattice codes. IEEE Trans Inf Theory, 2003, 49: 1385–1399
23 Farid A A, Hranilovic S. Channel capacity and non-uniform signalling for free-space optical intensity channels. IEEE J Sel Areas Commun, 2009, 27: 1553–1563

24 Li X, Vucic J, Jungnickel V, et al. On the capacity of intensity-modulated direct-detection systems and the information rate of ACO-OFDM for indoor optical wireless applications. IEEE Trans Commun, 2012, 60: 799–809
25 Betke U, Henk M. Intrinsic volumes and lattice points of crosspolytopes. Monatsh Mathematik, 1993, 115: 27–33

Appendix A Proof of Lemma 1

Consider the signal constellation defined as $\mathbf{X}=\{\mathbf{x}_m : m\in M\}$. For each transmitted signal, we let $\overline{\boldsymbol{\varphi}}_m=\{\bar{\varphi}_{n,m}, n\in N\}$, $m\in M$ be a set of real orthonormal basis functions. Then, the signal can be represented as combinations of the functions in N-dimension space:

$$\mathbf{x}_m=\sum_{n=1}^{N}\overline{x}_{m,n}\overline{\varphi}_{m,n}. \tag{A1}$$

For the combined signal, we write each signal symbol in the vector form as

$$\overline{\mathbf{v}}_m=\left[\bar{v}_{1,m},\cdots,\bar{v}_{N,m}\right],$$

and define the basis function as

$$\overline{\boldsymbol{\varphi}}_m=\frac{1}{\sqrt{T}}[\underbrace{1,0,\cdots,0}_{N}].$$

This choice can make the basis function contain the average amplitude, i.e., the average optical power of each signal [22]. Then, the peak-power constraint can be rewrite in terms of the signal-space definition by

$$0\leqslant\langle\overline{\mathbf{v}}_m,\overline{\boldsymbol{\varphi}}_m\rangle=\frac{\bar{v}_{1,m}}{\sqrt{T}}\leqslant HA, \tag{A2}$$

where the $\langle\cdot,\cdot\rangle$ operation is the Euclidean inner product of two vectors [22].

In a similar fashion, we can define the other basis vector:

$$\boldsymbol{\Psi}=\frac{1}{\sqrt{M}}\underbrace{[\underbrace{1,0,\cdots,0}_{N},\cdots,\underbrace{1,0,\cdots,0}_{N}]}_{MN},$$

and the signal constellation:

$$\boldsymbol{V}=[\boldsymbol{v}_1,\cdots,\boldsymbol{v}_M].$$

In addition, we assume the probability of each symbol is equal for a fixed symbol period T and the probability is $p(m)$. Then, the average-power constraint can be redefined as

$$\sum_{m=1}^{M}p(m)\,\mathbf{v}_m=\frac{1}{M}\sum_{m=1}^{M}\bar{v}_{1,m}\leqslant HP_0\sqrt{T}, \tag{A3}$$

or

$$\langle\boldsymbol{V},\boldsymbol{\Psi}\rangle\leqslant HP_0\sqrt{MT}. \tag{A4}$$

The admissible region of combined codewords can be expressed:

$$\Omega=\left\{\boldsymbol{V}\in\mathbb{R}^{MN}:0\leqslant\sum_{m=1}^{M}\bar{v}_{1,m}\leqslant MHA\sqrt{T},\langle\boldsymbol{V},\boldsymbol{\Psi}\rangle\leqslant HP_0\sqrt{MT}\right\}. \tag{A5}$$

The received region can be defined as[1)]

$$K=\left\{\boldsymbol{V}+\mathbf{Z}|\,\boldsymbol{V}\in\Omega,\mathbf{Z}\in rB^{MN}\right\}=\Omega\oplus rB^{MN}, \tag{A6}$$

where the $\oplus$ operation is the Minkowski addition of two sets[2)], and the set of K is the outer parallel body of Ω at distance r.

The received vector $\boldsymbol{Y}$ is conditionally Gaussian distributed with mean $\boldsymbol{V}$ and variance equals to σ^2. By the weak law of large numbers, as $M\to\infty$, the probability that all of the mass of the distribution of $\boldsymbol{Y}$ lies on K will be large enough[1)].

Define such two sets:

$$\boldsymbol{\Theta}_i=\{(v_1,v_2,\cdots,v_{MN})\in\Omega:v_i=0\},$$

and

$$\boldsymbol{\Phi}_i=\left\{\boldsymbol{Z}_i\boldsymbol{\Phi}:\boldsymbol{\Phi}=[\overline{\boldsymbol{\varphi}}_1,\cdots,\overline{\boldsymbol{\varphi}}_M]^{\mathrm{T}},\boldsymbol{Z}_i=\mathrm{diag}\,[z_1,\cdots,z_{MN}]\right\},$$

where the $[\cdot]^{\mathrm{T}}$ operation is the transposition of a vector, $i=kN+1,k=0,1,\cdots,(M-1)$,

$$z_j=\begin{cases}0,\ j=i,\\ 1,\ \text{otherwise.}\end{cases}$$

1) Schneider R. Convex Bodies: the Brunn-Minkowski Theory. 2nd ed. New York: Cambridge University Press, 2013. 128.

2) Vora P L. Inner products and orthogonality in color recording filter design. IEEE Trans Image Process, 2001, 10: 632–642.

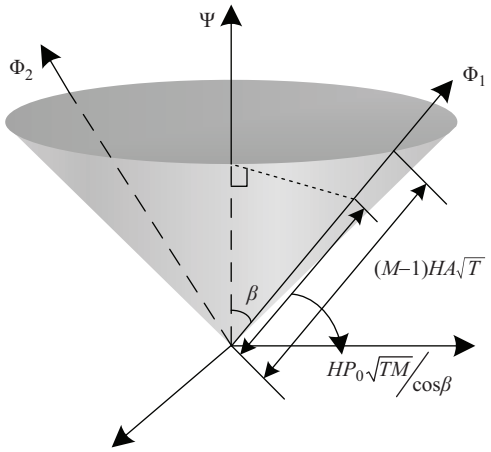

Figure A1 Two-dimensional $\boldsymbol{\Psi}$- and $\boldsymbol{\Phi}$-coordinates and representation of the admissible region Ω.

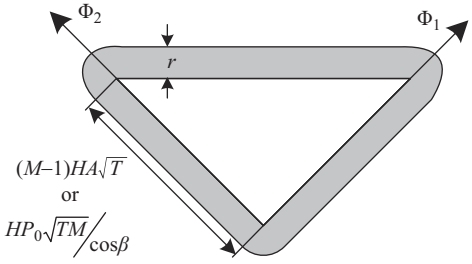

Figure A2 The parallel body of Ω at distance r, i.e., K.

Clearly, the set $\boldsymbol{\Theta}_i$ can be seen as a surface with the normal vector $\boldsymbol{\Phi}_i$ and $\langle \boldsymbol{V}, \boldsymbol{\Phi}_1 \rangle \leqslant (M-1)\, HA\sqrt{T}$. Define $\mathrm{O}_{\boldsymbol{\Theta}_i}$ and $\mathrm{O}_{\boldsymbol{\Phi}_i}$ are the projections of $\boldsymbol{\Psi}$ into $\boldsymbol{\Theta}_i$ and $\boldsymbol{\Phi}_i$, respectively, and unit vectors $\overline{\mathrm{O}}_{\boldsymbol{\Phi}_i}$ and $\overline{\mathrm{O}}_{\boldsymbol{\Theta}_i}$ as unit vectors of $\mathrm{O}_{\boldsymbol{\Phi}_i}$ and $\mathrm{O}_{\boldsymbol{\Theta}_i}$. The angle α between $\boldsymbol{\Psi}$ and $\overline{\mathrm{O}}_{\boldsymbol{\Phi}_i}$ and the angle β between $\boldsymbol{\Psi}$ and $\overline{\mathrm{O}}_{\boldsymbol{\Theta}_i}$ can be expressed as [16]

$$\cos\alpha = \begin{cases} \sqrt{\dfrac{M-1}{M}}\,, & i = kN+1,\ k = 0, 1, \cdots, (M-1)\,, \\ 1\,, & \text{otherwise}, \end{cases} \tag{A7}$$

$$\cos\beta = \begin{cases} \dfrac{1}{\sqrt{M}}\,, & i = kN+1,\ k = 0, 1, \cdots, (M-1)\,, \\ 0\,, & \text{otherwise}, \end{cases} \tag{A8}$$

and $\alpha + \beta = \frac{\pi}{2}$.

To analyze the problem more clearly, Figure A1 presents an example $M = 2$. The values of average-power and peak-power constraints can be found in $\boldsymbol{\Psi}$- and $\boldsymbol{\Phi}$-coordinates, respectively. The boundaries in $\boldsymbol{\Phi}_i$ are decided by one of two factors — the projection of $HP_0\sqrt{MT}$ in $\boldsymbol{\Psi}$ into $\boldsymbol{\Phi}_i$ or the values of $(M-1)\, HA\sqrt{T}$ in $\boldsymbol{\Phi}_i$. Thus, two situations need to be discussed in $\boldsymbol{\Phi}$-coordinate, which are

$$\frac{HP_0\sqrt{MT}}{\cos\beta} < (M-1)\, HA\sqrt{T} \tag{A9}$$

and

$$\frac{HP_0\sqrt{MT}}{\cos\beta} \geqslant (M-1)\, HA\sqrt{T}. \tag{A10}$$

Substituting the power ratio ρ and $M \to \infty$, the two ranges also can be denoted as $0 < \rho < 1$ and $\rho = 1$. The cross section of Ω and the corresponding received region K are shown in Figure A2.

Appendix B Proof of (14)

The following two results are used in the derivation of (14):

(1) the improper integral of the exponential function e^{-x^2}:

$$\int_0^\infty \mathrm{e}^{-x^2}\, dx = \frac{\sqrt{\pi}}{2}; \tag{B1}$$

(2) the error function inequalities:

$$\frac{1}{2} \leqslant \frac{1 + \mathrm{erf}\,(x)}{2} \leqslant 1,\ x \geqslant 0. \tag{B2}$$

For $0 \leqslant i \leqslant MN-1$,

$$\begin{aligned} \binom{MN}{i} \frac{1}{2^{MN-i}} &= \binom{MN}{i} \frac{1}{2^{MN-i-1}} \frac{1}{\sqrt{\pi}} \int_0^\infty \mathrm{e}^{-x^2}\mathrm{d}x \\ &= \binom{MN}{i} \frac{\sqrt{i+1}}{\sqrt{\pi}} \int_0^\infty \frac{1}{2^{MN-i-1}} \mathrm{e}^{-(i+1)t^2}\mathrm{d}t \\ &\leqslant \binom{MN}{i} \frac{i+1}{\sqrt{\pi}} \int_0^\infty e^{-(i+1)t^2} \left(\frac{1 + \mathrm{erf}\,(t)}{2}\right)^{MN-i-1} \mathrm{d}t. \end{aligned} \tag{B3}$$

Therefore, κ_i can be upper bounded as

$$\begin{aligned}\kappa_i &\leqslant \left[\binom{MN}{i}+\binom{MN}{i+1}\right]\frac{i+1}{\sqrt{\pi}}\int_0^{\infty}\mathrm{e}^{-(i+1)t^2}\left(\frac{1+\mathrm{erf}\,(t)}{2}\right)^{MN-i-1}\mathrm{d}t\\ &=\binom{MN+1}{i+1}\frac{i+1}{\sqrt{\pi}}\int_0^{\infty}\mathrm{e}^{-(i+1)t^2}\left(\frac{1+\mathrm{erf}\,(t)}{2}\right)^{MN-i-1}\mathrm{d}t\\ &\leqslant\binom{MN+1}{i+1}\frac{i+1}{\sqrt{\pi}}\int_0^{\infty}\mathrm{e}^{-(i+1)t^2}\mathrm{d}t\\ &=\binom{MN+1}{i+1}\frac{\sqrt{i+1}}{2}.\end{aligned}\tag{B4}$$

Appendix C Proof of (15c)

For $n\in\mathbb{R}^+$, the following results are true[3)]

(1) the Stirling-type formulas:

$$\mathrm{a}^{-\mathrm{a}}\mathrm{e}^{-n}(n+\mathrm{a})^{n+\mathrm{a}}\leqslant\Gamma\,(n+1)\leqslant\mathrm{c}^{-\mathrm{c}}\mathrm{e}^{-n}(n+\mathrm{c})^{n+\mathrm{c}};\tag{C1}$$

(2) the gamma function inequalities:

$$(\mathrm{a}+1)^{-(\mathrm{a}+1)}\mathrm{e}^{1-n}(n+\mathrm{a})^{n+\mathrm{a}}\leqslant n!\leqslant(\mathrm{b}+1)^{-(\mathrm{b}+1)}\mathrm{e}^{1-n}(n+\mathrm{b})^{n+\mathrm{b}},\tag{C2}$$

where $\mathrm{a}=1/2$, $\mathrm{b}=\mathrm{e}^{1-\gamma}-1$, $\mathrm{c}=\mathrm{e}^{-\gamma}$, γ is the Euler-Mascheroni constant.

Substituting into (15b) results in:

$$\begin{aligned}f_i\frac{\sqrt{i+1}}{2r^i i!}\frac{V\left(B^{MN-i}\right)}{V\left(B^{MN}\right)}&=\frac{(MN+1)!\left(MHP_0\sqrt{T}\right)^i(i+1)^{\frac{1}{2}}}{2i!\,(i+1)!\,(MN-i)!(\sigma^2MN)^{\frac{i}{2}}}\frac{\pi^{\frac{MN-i}{2}}\Gamma\left(\frac{MN}{2}+1\right)}{\Gamma\left(\frac{MN-i}{2}+1\right)\pi^{\frac{MN}{2}}}\\ &\leqslant\underbrace{\frac{\mathrm{c}^{-\mathrm{c}}(\mathrm{b}+1)^{-(\mathrm{b}+1)}}{2\mathrm{e}^2\mathrm{a}^{-\mathrm{a}}(\mathrm{a}+1)^{-3(\mathrm{a}+1)}}(MN+1+\mathrm{b})^{1+\mathrm{b}}\left(\frac{MN}{2}+\mathrm{c}\right)^{\mathrm{c}}}_{\xi_1(MN)}\\ &\quad\times\underbrace{\left(\frac{MN+1+\mathrm{b}}{MN-i+\mathrm{a}}\right)^{MN}\left(\frac{MN+2\mathrm{c}}{MN-i+2\mathrm{a}}\right)^{\frac{MN}{2}}\left(\frac{M}{i+\mathrm{a}}\right)^i}_{\xi_2(MN,i)}\\ &\quad\times\underbrace{\left(\frac{HP_0\sqrt{\mathrm{e}T}}{\sigma\sqrt{\pi}}\right)^i\left(\frac{MN-i+\mathrm{a}}{i+1+\mathrm{a}}\right)^i\left(\frac{(MN-i)/2+\mathrm{a}}{MN}\right)^{i/2}}_{\xi_3(MN,i)}\\ &\quad\times\underbrace{\frac{(i+1)^{1/2}((MN-i)/2+\mathrm{a})^{-\mathrm{a}}}{(i+\mathrm{a})^{\mathrm{a}}(i+1+\mathrm{a})^{1+\mathrm{a}}(MN-i+\mathrm{a})^{\mathrm{a}}}}_{\xi_4(MN,i)}.\end{aligned}\tag{C3}$$

Then, the upper bound can be transformed into

$$C\leqslant\lim_{M\to\infty}\frac{1}{M}\log_2\frac{V(\Theta)}{r^{MN}\cdot V\left(B^{MN}\right)}\tag{C4a}$$

$$\leqslant\lim_{M\to\infty}\frac{1}{M}\log_2\left\{\sum_{\substack{i=kN+1\\k=0,1,\cdots,(M-1)}}\left[\xi_1(MN)\,\xi_2(MN,i)\,\xi_3(MN,i)\,\xi_4(MN,i)\right]\right\}\tag{C4b}$$

$$\leqslant\lim_{M\to\infty}\frac{1}{M}\log_2\left\{M\cdot\max_i\left[\xi_1(MN)\,\xi_2(MN,i)\,\xi_3(MN,i)\,\xi_4(MN,i)\right]\right\}\tag{C4c}$$

$$=\max_i\lim_{M\to\infty}\frac{1}{M}\log_2\left[\xi_2(MN,i)\,\xi_3(MN,i)\right].\tag{C4d}$$

The derivation of (C4d) can be seen in Appendix D.

Define

$$F_1(MN)=\xi_2(MN,i)\,\xi_3(MN,i).$$

Then, the result (15c) can be verified.

3) Batir N. Inequalities for the gamma function. Arch Math, 2008, 91: 554–563.

Appendix D Proof of (C4d)

The limits of the following functions are true:

$$\lim_{x\to\infty}\frac{1}{x}\log_2 \mathrm{a}=0,$$

and

$$\lim_{x\to\infty}\frac{1}{x}\log_2(x+\mathrm{a})^{\mathrm{b}}=\lim_{x\to\infty}\log_2(x+\mathrm{a})^{\frac{\mathrm{b}}{x}}=\lim_{x\to\infty}\log_2 \mathrm{e}^{\frac{\mathrm{b}}{x}\ln(x+\mathrm{a})}=\lim_{x\to\infty}\log_2 \mathrm{e}^{\frac{\mathrm{b}}{x+\mathrm{a}}}=1.$$

Therefore, we can get

$$\lim_{M\to\infty}\frac{1}{M}\log_2\xi_1\left(MN\right)=0.$$

Define $i=\lfloor u\left(M-1\right)\rfloor N+1$, then

$$\begin{aligned}&\lim_{M\to\infty}\frac{1}{M}\log_2\xi_4\left(MN\right)\\&=\lim_{M\to\infty}\frac{1}{M}\log_2\left\{\frac{\left(uMN-uN+2\right)^{\frac{1}{2}}}{\left(uMN-uN+1+\mathrm{a}\right)^{\mathrm{a}}}\frac{\left[\frac{\left(1-u\right)MN+uN}{2}+\mathrm{a}\right]^{-\mathrm{a}}\left[\left(1-u\right)MN+uN-1+\mathrm{a}\right]^{-\mathrm{a}}}{\left(uMN-uN+2+\mathrm{a}\right)^{1+\mathrm{a}}}\right\}\\&=0.\end{aligned}$$

Therefore, (C4d) can be verified.

Appendix E Proof of corolloary 1

E.1 High-SNR asymptotic expressions

At high SNR, $u^*\to 1$ and the analysis of the asymptotic upper bound (26) can be solved.

E.2 Low-SNR asymptotic expressions

Based on the rate of convergence of power function, for $0<x<1$ and $0<i<j$, x^i decreases faster to 0 than x^j, i.e.,

$$\lim_{x\downarrow 0}\frac{x^j}{x^i}=0.$$

At low SNR, $u^*\downarrow 0$. To find a suitable asymptotic expansion, we consider one value decreases slower to 0 than $\mathrm{C_{UB}}$ does. In (24), all items can be rewritten as

$$u^*=\sum_i a_i d_0^{n_i},\tag{E1}$$

where a_i and n_i are the coefficient and the exponent of the i-th item, and the maximum and minimum values of n_i are 2 and $\frac{1}{3}$, respectively.

Then, the first part in (25) satisfies

$$\begin{aligned}&\lim_{d_0\downarrow 0}\frac{Nu^*\log_2 d_0}{d_0^{1/3}}=\lim_{d_0\downarrow 0}\frac{N\log_2 d_0\sum_i a_i d_0^{n_i}}{d_0^{1/3}}=\lim_{d_0\downarrow 0}\frac{N\left(\sum_i a_i d_0^{n_i}\right)^2}{d_0\left(\frac{d_0^{-2/3}}{3}\sum_i a_i d_0^{n_i}-d_0^{1/3}\sum_i a_i n_i d_0^{n_i-1}\right)}\\&=\lim_{d_0\downarrow 0}\left[-\frac{3N\left(\sum_i a_i d_0^{n_i}\right)^2}{2\sum_i a_i d_0^{n_i+1/3}}\right]=0.\end{aligned}\tag{E2}$$

The second part in (25) satisfies

$$\lim_{d_0\downarrow 0}\frac{\frac{3N}{2}\left(u^*-1\right)\log_2\left(1-u^*\right)}{d_0^{1/3}}=\lim_{d_0\downarrow 0}\frac{\frac{3N}{2}\log_2\left(1-\sum_i a_i d_0^{n_i}\right)}{d_0^{1/3}\Big/\left(\sum_i a_i d_0^{n_i}-1\right)}=0.\tag{E3}$$

The third part in (25) satisfies

$$\lim_{d_0\downarrow 0}\frac{-2Nu^*\log_2\left(u^*\right)}{d_0^{1/3}}=\lim_{d_0\downarrow 0}\frac{-2N\log_2\left(\sum_i a_i d_0^{n_i}\right)}{d_0^{1/3}\Big/\left(\sum_i a_i d_0^{n_i}\right)}=0.\tag{E4}$$

Then, the asymptotic upper bound (27) can be solved.